Conformational Properties of the Bacterial Polyester Poly(3-hydroxy-5,8-decadienoate)

Serdal Kirmizialtin,[†] Canan Baysal,*[,†] and Burak Erman[†,‡]

Faculty of Engineering and Natural Sciences, Sabanci University, Orhanli 81474, Tuzla, Istanbul, Turkey, and Departments of Chemistry and Mechanical Engineering, Koc University, Rumelifeneri Yolu 80910, Sariyer, Istanbul, Turkey

Received July 11, 2002; Revised Manuscript Received November 27, 2002

ABSTRACT: Molecular dynamics simulations under different conditions and rotational isomeric states calculations are performed to understand the local and global conformational properties of the bacterial polyester poly(3-hydroxy-5,8-decadienoate). The rotational isomeric state model is incorporated with Monte Carlo simulations to calculate the dimensions and the characteristic ratio of the infinitely long chain. These calculations, performed in a vacuum, predict a Gaussian distribution for the end-to-end vector with a nonzero mean and a value of 5.5 for the characteristic ratio. Molecular dynamics simulations predict the characteristic ratio of the single chain in good solvent as 23. The role of temperature on the overall dimensions and on the distribution of dihedral angles is discussed. Radii of gyration and helix formation propensities at different temperatures and in different media are compared. The chain in solution is found to have the largest persistence length with the highest helical persistence. Results are compared with experimental and theoretical studies conducted on poly(3-hydroxybutyrate), which has the same backbone structure but a different type of side chain.

Introduction

Bacterial polyesters are naturally occurring polymers which act as important storage materials in a variety of bacteria. Elementary analysis, infrared spectroscopy, autolysis, saponification, and degradation experiments all support a linear head-to-tail polyester structure with the general formula[1]

$$-O-C(HR_1)-C(R_2R_3)-CO-$$

where R_1, R_2, and R_3 are the side groups. The functional units of the above polyesters, which have the generic name of poly(hydroxy alkanoate)s (PHAs), are determined by the bacterial species and feedstock. By this means, PHAs with improved physical features can be produced. The current state of understanding of PHAs has recently been presented by Marchessault and Yu.[2] These polymers (i) are biodegradable in water and carbon dioxide,[3] (ii) are thermoplastic, and (iii) act as a carbon and energy reserve.[4] Therefore, they are foreseen as clean alternatives of many industrially important polymers such as polypropylene. However, they are unstable at processing temperatures and have poor mechanical properties for industrial applications. To remedy these problems, copolymers of certain biopolyesters have been synthesized. For example, poly(3-hydroxybutyrate-*co*-3-hydroxyvalerite), Biopol, has achieved a limited industrial application.[3,4]

Among the large class of biopolyesters, the conformational properties and local chain dimensions in different environments of poly(3-hydroxybutyrate), PHB, have been extensively studied. The solid-state properties of PHB were first studied by Cornibert et al.[1] Their X-ray analysis showed that PHB crystallizes into a left-handed 2_1-helix with two unparallel chains packed in an orthorhombic unit cell. These authors have proposed that the backbone dihedrals have repeated stretches of the states ttg^+g^+, where g^+ is approximately perpendicular to the fiber axis. The ester bond, on the other hand, was observed to have a small deviation from planarity. They reported the angle between the dipoles of the ester groups as ∼60° in the unit cell and suggested that dipole−dipole interactions were the main factor determining the packing and the overall conformation.

Brückner et al.[5] undertook both isotactic and lower tacticity racemic polymers of PHB and observed results similar to the previous study with an extra refinement of the unit cell parameters. In another study, Pazur and co-workers[4] have employed molecular modeling and X-ray fiber diffraction techniques to investigate the crystalline chain conformations of a series of PHBs. Among the minimum-energy conformations, a left-handed 2_1-helix with lattice parameters similar to the X-ray data of Brückner's study was reported for the iso-PHB.

Solution properties of PHB were studied by intrinsic viscosity, sedimentation analysis, and optical rotary dispersion experiments (ORD) by Marchessault and Okamura.[6] Viscometry and ORD experiments performed in chloroform indicated partially rodlike linear chains. The chain size was found to have a minor effect on the conformation. Depending on the solvent type and temperature, either randomly coiled or partially helical segments were proposed. As the solvent composition and temperature changed, a sharp helix−coil transition similar to that observed in proteins occurred. Miyaki et al. subsequently studied the dilute solution properties of a series of fractionated PHBs by light scattering and viscosity experiments.[7] They were unable to reproduce the ORD observations of Marchessault and Okamura which had suggested a propensity to the helices in some solutions. Instead, they reported a randomly coiling structure in dilute solution of good solvents such as

[†] Sabanci University.
[‡] Koc University.
* Corresponding author: phone +90 (216) 483 9523; Fax +90 (216) 483 9550; e-mail canan@sabanciuniv.edu.

10.1021/ma021088z CCC: $25.00
Published on Web 01/31/2003

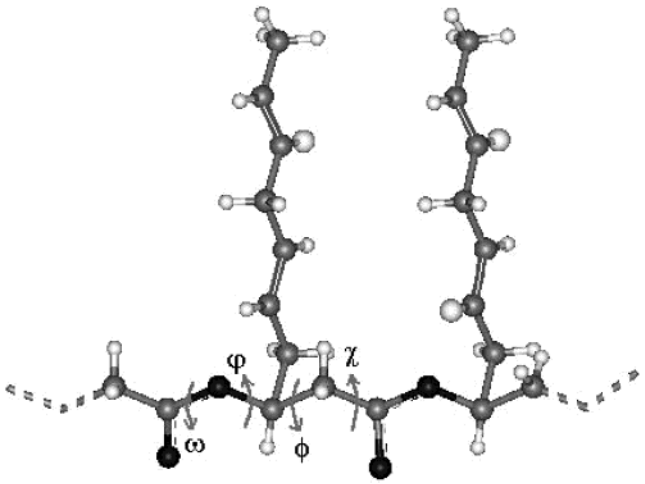

Figure 1. Two repeat units of the aliphatic polyester isotactic PHD with the bulky side chains of $CH_2-(CH)_2-CH_2-(CH)_2-CH_3$. ω, φ, ϕ, and χ denote the internal rotational angles of the backbone. The double bonds in the side chains are in their trans configurations.

2,2,2-trifluoroethanol (TFE). In addition, when their data are extrapolated to the unperturbed state, the characteristic ratio, C_∞, is found as ca. 8.

The unperturbed dimensions of PHB in the nonsolvent TFE/water were studied by Huglin et al.[8] They reported unperturbed dimensions, $(\langle r^2\rangle_0/M)^{1/2}$, as 0.085 $nmg^{-1/2}$ $mol^{1/2}$, where $\langle r^2\rangle_0$ is the mean-square end-to-end distance and M is the molar mass. If the square of the average bond length, $\langle l^2\rangle$, is taken as 2.07 Å^2 with the repeat unit molecular weight of 86 g/mol, then C_∞ is calculated as ca. 7.5 from these experiments. Beaucage et al.,[9] on the other hand, observed a high degree of local chain persistence and unusual rheology for iso-PHB in the amorphous state. The C_∞ in the amorphous state was found to be ca. 40 from the persistence length measurements using both SANS and rheology experiments. The studies reviewed above reveal that experimental results are open to interpretations, and there are controversies about the chain dimensions in the unperturbed state and the existence of helical segments in solution. A detailed analysis of conformational properties will lead to a better understanding of these experiments.

One of the few studies of the conformational properties of PHAs is by Marchessault and collaborators.[4] In their molecular mechanics study, helical propensities of PHB as well as other short side-group PHAs such as poly(3-hydroxybutyrate-*co*-3-hydroxyvalerate), poly(4-hydroxybutyrate), and poly(tetramethylenesuccinate) were determined. Results showed a strong tendency to form helical structures in the minimum-energy conformation. This was also verified by experiments.[6] These chains exhibit various degrees and types of crystallinity in the bulk state, depending on their chemical identity and the type and location of their side groups. In the present paper, we study the conformational characteristics of a different class of PHA, namely poly(3-hydroxy-5,8-decadienoate) (PHD), where the side groups R_2 and R_3 are hydrogens and R_1 is an aliphatic long chain, $CH_2-(CH)_2-CH_2-(CH)_2-CH_3$ (Figure 1). The relatively large size and flexibility of the side groups introduce significant entropic effects to the statistics of these chains. Because of their large sizes, the side chains also cause considerable crowding. Hence, the conformational features of these molecules are expected to differ, especially with regard to unperturbed dimensions and helical propensities, from those of the PHBs studied earlier. In the interest of understanding the statistical properties of these chains, detailed molecular dynamics (MD) and Monte Carlo (MC) analysis of static and dynamic properties of PHD are performed at different temperatures and in different environments. The results are compared with those of PHBs.

Models and Methods

The Rotational Isomeric States Model. The dimensions of PHD chains were calculated by the rotational isomeric states (RIS) model. The structure of the dimer molecule shown in Figure 1 was energy minimized using the Polymer Consistent Force Field (PCFF)[10,11] implemented within the Molecular Simulations Inc. InsightII 98.0 software package, with a stringent minimization criterion of at least 10^{-3} kcal/(mol Å) of the derivative. During torsional angle variations, the valence angles and bond lengths were assumed to be fixed at the values of the minimized geometry. Long-range interactions are ignored by considering only the nonbonded contributions from first-order interactions. A conformation of the chain is described by the four torsional angles ω, φ, ϕ, and χ (Figure 1). The energies corresponding to the three rotational pairs, i.e., (ω, φ), (φ, ϕ), and (ϕ, χ), were calculated by 1° increments of the torsional angles. Energy calculations were performed with no minimization and no cutoff. The relative population of the rotamers, γ, was calculated with the Boltzmann weight formula as $\gamma = \exp[-E(\theta_1,\theta_2)/RT]$, where $E(\theta_1,\theta_2)$ represents the energy as a function of the rotational angle pair (θ_1, θ_2). The MC chain generation technique with statistically weighted isomeric states was incorporated to generate chains for calculating chain dimensions. The chains are generated using the matrix multiplication methods given in ref 11. The end-to-end distance distribution of the unperturbed chains, $W(r)$, was fitted to a Gaussian distribution function of the form

$$W(r) = [A/(2\pi\sigma^2)^{1/2}] \exp[-{}^1/_2((r - \langle r\rangle)^2/\sigma^2)] \qquad (1)$$

Here, A is the normalization constant, σ is the standard deviation of the end-to-end distance, and $\langle r\rangle$ is the ensemble average of the end-to-end distance. To monitor the chain dimensions, the characteristic ratio of the chains for an infinitely long chain, defined by $C_\infty = \lim_{n\to\infty} \langle r^2\rangle/nl^2$, is calculated. Here, $\langle r^2\rangle$ is the ensemble average of the square of the end-to-end separation, n is the number of bonds, and l^2 is the square of the bond length. The persistence of an unperturbed chain is measured by the persistence length, l_p, where $l_p = l_k/2$. Here, l_k is the Kuhn length defined as $\langle r^2\rangle/r_{max}$.[12]

MD Simulations. We carried out MD simulations in a vacuum, in the bulk, and in chloroform solution, treating all atoms explicitly. The PHD molecule utilized in the vacuum simulations consists of 30 monomer units and has an initially extended structure with an end-to-end distance of ca. 122 Å. A time step of 0.5 fs was used, and the temperature was kept fixed at the desired value by using the temperature control method of Andersen.[13,14] Initial velocities were generated from a Boltzmann distribution, and integration was carried out by the velocity Verlet algorithm.[15] Group-based cutoffs were used with a 9.5 Å cutoff distance; a switching function was used with the spline and buffer widths set to 1.0 and 0.5 Å, respectively. The neighbor list was updated whenever any atom moved more than one-half the buffer width. The PCFF parameters were used for energy calculation. The positions of the atoms were recorded every 2 ps for further analysis. In the first part of the MD calculations, the behavior of the single chain in a vacuum at the temperatures of 250, 300, 350, and 400 K was analyzed. All of the geometries were optimized by the conjugate gradients method up to a final convergence of 0.1 kcal/(mol Å). After generation and minimization of all the systems, dynamic calculations were performed with 50 ps equilibration followed by a 1.0 ns data collection stage.

For the simulation in good solvent, a 30-repeat-unit chain of PHD, for which the pair of atoms that are farthest apart from each other are at a 86 Å distance, was immersed in a cubic box of 52 Å dimensions with 1000 chloroform ($CHCl_3$) molecules in it. This corresponds to a density of 1.49 g/cm^3, which is the experimentally measured density of chloroform. The initial configuration of the chain was fitted into the cube along the diagonal, which is 90 Å long. We check that the chain remains within the cube throughout the simulations. Periodic boundary conditions were applied with a cutoff radius of 9.5 Å for all nonbonded interactions, and van der Waals tail corrections were taken into account.[15] The initially packed cell was optimized by first the steepest descents and then conjugate gradients methods up to a final convergence of 0.05 kcal/(mol Å) of the derivative. To remove bad contacts, the system was refined by an NVT simulation at 300 K, where the temperature was controlled for 0.1 ns by velocity rescaling followed by 0.4 ns of Nosé protocol.[16] After equilibration was reached, 1.7 ns of MD simulation was performed with the Andersen temperature control method at the same temperature. In all simulations, the various quantities investigated were calculated from the portion of the MD trajectories for which equilibrium has been reached.

Results and Discussion

RIS Model Results. The overall dimensions of a chain depend strongly on the conformation of the backbone atoms. The backbone of the PHD molecule has four bond vectors. The partial double bond nature of the ester bond, shown in Figure 1, restricts the rotation angle ω to the trans state (0° in Flory representation[11]). We carried out single-point energy calculations for every increment of rotation between the pairs (ω, φ), (φ, ϕ), and (ϕ, χ) as labeled in Figure 1. The rigid rotor approximation was used for the rotatable bonds, and fluctuations in the bond stretching and bending degrees of freedom were ignored. To simplify the model, the four different bond lengths and valence angles were averaged over the optimum geometry of the dimer molecule. This gives $\langle l^2 \rangle$ as 2.07 Å^2 and the valence angle as 114°. The torsional states t, g^-, and g^+ for each bond were obtained from the energy surfaces expressed in terms of torsional angle pairs, similar to the case of the polyethylene model. The rotational minima for the three states t, g^-, and g^+ exhibited shifts of ±20 from the ideal gauche and trans values. In particular, the trans state of the φ torsion occurs at 40 ± 10°. The population matrices constructed for the RIS model from the conformational energies are as follows:

$$\mathrm{P}(\omega,\varphi) = \begin{array}{c} \\ t \end{array} \begin{array}{c} \begin{array}{ccc} t & g^- & g^+ \end{array} \\ \begin{bmatrix} 0.7320 & 0.0005 & 0.2675 \end{bmatrix} \end{array}$$

$$\mathrm{P}(\varphi,\phi) = \begin{array}{c} t \\ g^- \\ g^+ \end{array} \begin{array}{c} \begin{array}{ccc} t & g^- & g^+ \end{array} \\ \begin{bmatrix} 0.1276 & 0.2496 & 0.0912 \\ 0.0238 & 0.0086 & 0.0000 \\ 0.2496 & 0.2496 & 0.0000 \end{bmatrix} \end{array}$$

$$\mathrm{P}(\phi,\chi) = \begin{array}{c} t \\ g^- \\ g^+ \end{array} \begin{array}{c} \begin{array}{ccc} t & g^- & g^+ \end{array} \\ \begin{bmatrix} 0.0000 & 0.1630 & 0.2280 \\ 0.0000 & 0.1630 & 0.4460 \\ 0.0000 & 0.0000 & 0.0000 \end{bmatrix} \end{array}$$

Note that our detailed calculations and comparisons with the populations obtained from the MD calculations in a vacuum showed that the position dependence of the population matrices was a second-order effect. We therefore used the same population matrices for all positions along the chain for the MC calculations.

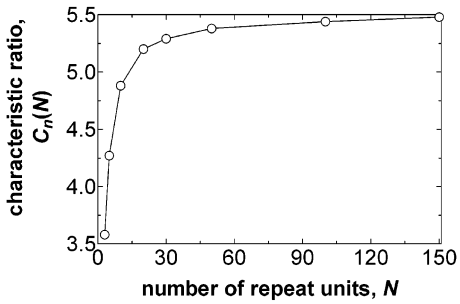

Figure 2. Characteristic ratio, $\langle r^2 \rangle / nl^2$, of the PHD chain of various sizes, calculated by the RIS model at 300 K. A line is drawn through the points to guide the eye. Only the short-range interactions are considered for chain growth to predict the unperturbed dimensions of the PHD chain. The value converges to the infinitely long chain as the chain size increases. The 30 repeat unit polymer, for which C_n is 95% of C_∞ and is computationally manageable in size, is taken as the representative chain in all the subsequent calculations.

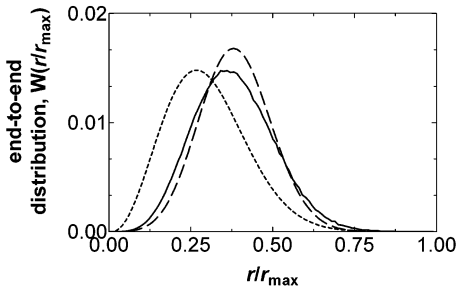

Figure 3. Distribution of normalized end-to-end distance of 150 repeat unit PHD chain generated by the RIS method (—) and fitted to a Gaussian distribution with both nonzero (- - -) and zero mean (• • •), where "mean" refers to $\langle r \rangle$ in eq 1. Because of the large side chains, PHD shows persistence to higher dimensions with a nonzero mean.

Chain dimensions at different temperatures were analyzed with the MC chain generation technique as described above. In Figure 2, the characteristic ratio $C_n(N)$ is presented as a function of the number of repeat units. Here, n is the number of bonds in the backbone and N is the number of repeat units in a chain with $N = 4n$. The open circles represent results of calculations, and the curve through the points is drawn to guide the eye. The characteristic ratio, C_{120}, of the 30 repeat unit chain is 5.3 at 300 K and increases only very slightly as a function of chain length up to 5.5 for the 150 repeat unit chain. The C_{120} value is 95% of the asymptotic value for the PHD chain. For the range between 250 and 400 K, the temperature coefficient, on the other hand, is 1.3 $\times$ 10^{-3}. Note that the characteristic ratio for PHB in Θ solvent is ca. 7.5.[8] The chain dimensions r_{max}, $\langle r \rangle$, and $\langle r^2 \rangle$ for the 100 repeat unit chain are 218 Å, 63.4 Å, and 4512 Å^2, respectively. These values lead to the Kuhn length of 20.7 Å with 42 bonds in each Kuhn segment.

In Figure 3, the distribution of the normalized end-to-end distance, $W(r)$, of the 150 repeat unit chain as a function of normalized end-to-end separation is shown. Here, the distribution generated by the RIS method (solid line) is fitted to a Gaussian distribution with both nonzero mean (dashed) given in eq 1 and zero mean (dotted) defined by Flory.[12,17] The maximum in the distribution function shifts to the r/r_{max} ratio of 0.4, which is 0.25 for the ideal Gaussian chain with zero mean. The larger end-to-end distance is due to the long side chains and the partial double bond nature of the ester bond that leads to rotational hindrance.

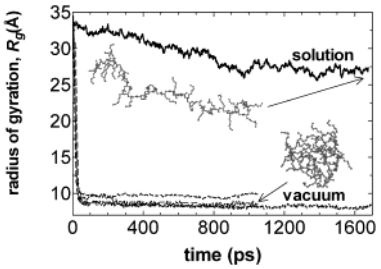

Figure 4. Radius of gyration of the backbone for the 30 repeat unit PHD chain as a function of time, calculated by MD simulations. Different runs are performed for PHD in chloroform solution at 300 K (1.7 ns) and in a vacuum at 250, 300, 350, and 400 K (1.1 ns for the former three, 1.7 ns for the latter). The initial geometry is a rodlike helix whose rotational angles are in the tg^+tg^+ state. In the vacuum, irrespective of temperature, a helix-to-coil transition occurs in ca. 50 ps. In chloroform, fluctuations are higher, and the overall geometry is in the vicinity of the initial structure. Snaphots of the structures at the end of the trajectories in a vacuum at 300 K and in chloroform are shown as an inset.

MD Simulation Results. a. Analysis of the Single Chain. To understand the conformational features of the PHD molecule, a dimer and a PHD chain with 30 repeat units were analyzed using MD simulations. The geometry of the dimer molecule, capped with H atoms at both ends, was optimized by carrying out a stringent minimization for each of the minima at the energy surface of the rotatable bond pairs discussed above. Detailed analysis of the conformational characteristics shows similarities with the theoretical studies performed for PHB. Marchessault and co-workers proposed the backbone dihedrals of the isotactic PHB as ttg^+g^+, whose repetition leads to helices.[4] They report a 3.0 Å helical rise per repeat unit. In our calculations for isotactic PHD, the rotational angles of the dimer (ω, φ, ϕ, χ) are 3.5°, 107.7°, 7.2°, and 93.2°, respectively, and conform to the tg^+tg^+ state. We calculate the end-to-end distance of a repeat unit as 4.4 Å and the helical rise per repeat unit as 3.9 Å. The more extended conformation of the backbone of PHD compared to that of PHB is attributed to the repulsive forces between adjacent bulky side chains. Our calculations also predict stretched out side chains in the anti configuration with an end-to-end distance of 7.6 Å.

By using these parameters, we generated the initial configuration of the PHD chain. The convergence of the characteristic ratio in the MC study lets us utilize 30 repeat units of PHD chain as a model throughout the MD simulations. This chain size is a good representative of the dimensions of an infinitely long chain and is small enough to feasibly execute the simulations. After energy minimization, the optimum geometry of the PHD chain results in rodlike helices with geometric parameters in the vicinity of the optimum dimer structure. At this local minimum the R_g and C_n are 34 Å and 44, respectively.

MD simulations of the single chain in a vacuum at different temperatures indicate a sharp transition from helical rodlike to a randomly coiled globular structure. Figure 4 shows the evolution of R_g at temperatures 250, 300, 350, and 400 K in a vacuum. This sharp transition is similar to the one observed in the ORD experiments when solvent quality decreases.[6] Independent of temperature, this transition occurs at around 50 ps. The calculated C_n values for the four simulations at 250−400 K lie in the range 0.3−1.6.

b. Analysis of the Effect of Chloroform Solution. MD simulations have been successful in calculating the unperturbed dimensions and C_∞ value of the poly(ethylene terephthalate) (PET) chains from the bulk state simulations.[18] Along similar lines, we analyzed the conformational features of 30 repeat unit long PHD molecules in chloroform. Periodic boundary conditions were applied in all directions so that the behavior of a sufficiently large system can be obtained. As shown in Figure 4, in chloroform solution, R_g converges in about 700 ps and fluctuations are higher than those found in the vacuum simulations. The chain shows a strong preference for a rodlike conformation with a R_g of 27 Å. This size is ca. 20% smaller than the R_g of the rodlike helical structure mentioned in the previous subsection. Finally, we observed C_∞ as 23 Å and l_p as 22 Å in solution. For PHB in the amorphous state, the C_∞ and l_p values were calculated as 18 and 19 Å, respectively. The chain dimensions of the amorphous PHB, on the other hand, was observed as 39 and 31 Å from SANS experiments.[9]

The results summarized above indicate that chain dimensions show differences depending on the environment. In a vacuum, attractive interactions are overemphasized, thus resulting in small chain dimensions compared with the solution environment. The temperature, on the other hand, has no significant influence on chain dimensions in a vacuum. The dimensions predicted by MD simulations in chloroform solution (a good solvent for PHD) are larger than those obtained from MC simulations.

Ideally, the chain behavior in the bulk state is representative of the unperturbed state. Thus, results from bulk simulations may be taken to correspond to chain behavior in Θ solvent. On the other hand, RIS calculations for which only the short-range interactions are taken into account should also represent the unperturbed state in principle. Thus, the prediction from the RIS model, $C_\infty = 5.3$, is in accord with the expectation from the MD simulations, ca. $1 < C_\infty < 23$ for the chain behavior at the Θ point. This is despite the incomplete treatment of the side chains in the RIS model: PHU chains have bulky side chains, but during MC chain generation the excluded-volume interactions among neighboring side chains are not considered, resulting in the estimation of lower chain dimensions in the RIS model.

c. Analysis of the Dihedral Angles. Among the three local geometric variables, the bond length, the valence angle, and the dihedral angle, only the dihedral angle has significant effects on the overall conformation of a chain. We find that the dihedral angle shows differences as the temperature and environment changes in the simulations. Therefore, a detailed analysis of dihedral angles leads to an understanding of the structural changes, the dynamics, and the flexibility of the chains. The roles of temperature and environment on the population of the rotational angles are investigated from the ensembles generated from the MD simulations. In all simulations, the partial double bonded ester bond is observed to be in the trans form with fluctuations around ±60°. This behavior is independent of the temperature and the environment. The populations of other dihedrals (φ, ϕ, χ), averaged over the last 500 ps of each trajectory, as a function of dihedral angle in degrees are summarized in Figures 5−7; we will elaborate on the details of these figures below. The effect of the environment (vacuum or solvated) at the constant temperature of 300 K is shown in the figures, whereas

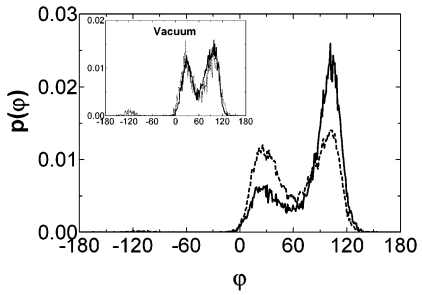

Figure 5. φ angle distribution calculated from MD simulations. In a vacuum at 300 K (- - -), t and g^+ states have equal probabilities, while in chloroform solution at 300 K (—) g^+ is favored. The inset shows the vacuum behavior of PHD at 250 K (—) and 400 K (· · ·); a minor population arises at the g^- state at higher temperatures.

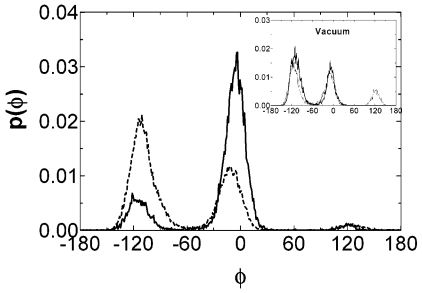

Figure 6. ϕ angle distribution calculated from MD simulations. In a vacuum at 300 K (- - -), g^- and t states are favored, while in chloroform solution (—) at 300 K (· · ·) the t state is predominant. The inset shows the vacuum behavior of PHD at 250 K (—) and 400 K (· · ·); at higher temperatures three states are populated while at low temperatures g^- and t are favored.

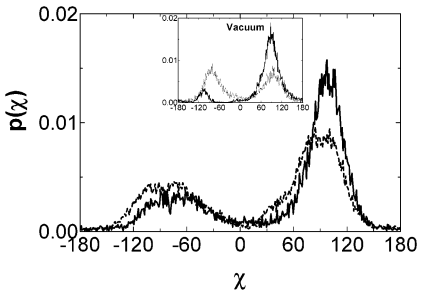

Figure 7. χ angle distribution calculated from MD simulations. In a vacuum at 300 K (- - -) and in chloroform solution at 300 K (—), g^+ and g^- are favored with a preference toward the former. The inset shows the vacuum behavior of PHD at 250 K (—) and 400 K (· · ·); the preference of the g^+ state at lower temperatures shifts toward an equal distribution of g^- and g^+ as the temperature is increased.

the temperature effect is displayed in the insets. Note that, since the behavior of the chain at 350 and 400 K is nearly the same for all four types of dihedral angles, only the results from the 400 K simulations are shown in these figures.

The rotation of the O−C bond, represented by the φ angle, varies as the conditions are changed. The RIS model estimates two predominant conformers, t and g^+, with populations 0.27 and 0.73, respectively. Similarly, all the MD simulations reflect the preference of the φ angle toward the t and g^+ states, as shown in Figure 5. As the temperature is changed from 250 to 400 K, the g^+ population is slightly reduced from 0.61 to 0.49; also, a slightly populated g^- state emerges at the higher temperatures (see inset of Figure 5). The role of the environment on the statistics of φ is more significant. In chloroform, where the g^- state is not populated, the dihedral distribution of φ shows a distinct preference for the g^+ state with a t:g^+ probability ratio of 0.25:0.75, very similar to the RIS model result.

We observe two dominant states for the ϕ angle in the MD simulations. The states t and g^- are the two minima that emerge in the probability matrix of the RIS calculations. These two minima are also significantly populated in the MD simulations (Figure 6). Here, the $g^- \leftrightarrow t$ transition occurs easily at every temperature and in every environment. In a vacuum, a slight preference for the g^- state is observed. In addition, at 250 K, the energy barrier to g^+ cannot be surmounted. As the temperature is increased, probabilities of the two states become closer to each other and the population of g^+ increases (inset of Figure 6). The environment again has a more pronounced effect on the population of the ϕ angle. In solution the t state is overpopulated, in contrast to the vacuum case. The probability of g^-:t in a vacuum is 0.76:0.22 while for the solution it is 0.17:0.81. Interestingly, in the RIS calculations, this ratio is 0.59:0.40; i.e., there is a slight preference to the g^- state.

The distribution of the χ angle, displayed in Figure 7, has two maxima at g^- and g^+ under all conditions. Because of its high energy, as corroborated by the RIS model, the t state is not populated. At 250 K, g^+:g^- has a ratio of 0.78:0.09, while as the temperature is increased to 400 K, this ratio changes to 0.45:0.46. Note that approximately 10% of the conformations lie in the range $-60° < \chi < 60°$ (inset of Figure 7). In addition, an increase in temperature results in a broadening of the available states. In comparing the distribution of χ in different environments, we observe that the distribution of χ in the solvent favors the g^+ state (Figure 7) with a g^-:g^+ ratio of 0.18:0.73. This ratio is 0.32:0.68 in the RIS calculations.

d. Helix Formation. The detailed study of rotational angles, outlined above, indicates that ω has access to the t state only, while each of the other three angles, φ, ϕ, and χ, may be found in two probable states. This results in eight different combinations of rotational angles (ω, φ, ϕ, χ) for the backbone of the PHD molecule: $tttg^-$, $tttg^+$, ttg^-g^-, ttg^-g^+, tg^+tg^-, tg^+tg^+, $tg^+g^-g^-$, $tg^+g^-g^+$. If any of these combinations repeats persistently along the chain, a helical structure will emerge; otherwise, a randomly coiling structure is expected. To comprehend the helicity of the chain, we recorded the number of times these combinations repeat along the backbone. From the eight conformations, only the combination tg^+tg^+ occurs more than 1% during the simulation. We define the helix length as the consecutive number of repetitions of the tg^+tg^+ state, given as percent of the total chain length. We also define helix persistence as the percent of simulation time during which a certain helix length is observed in the trajectory. To remove end effects, two repeat units from each end are discarded. Results for different temperatures and environments are summarized in Figure 8. Here, the helix persistence as a function of helix length is shown for PHD chains of 30 repeat units. The labels on the figure represent the environment or the temperature of the simulations. The "solution" label represents the chain behavior in chloroform solution at 300 K. The other labels (250, 300, 350, and 400 K) represent the behavior of chain in a vacuum at the specified temperature. Curves are drawn through the points to guide

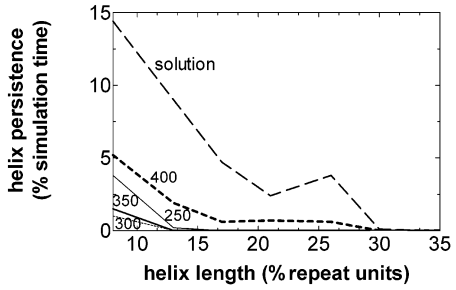

Figure 8. Helix persistence as a function of helix length calculated from MD simulations for PHD chains of 30 repeat units at different temperatures and in different environments. In a vacuum, irrespective of temperature, helix formation is not significant. In chloroform, which is representative of a good solvent for PHD, the chain has considerable helix persistence.

the eye. Here, we see an insignificant amount of helix formation at all temperatures in a vacuum. In solution, longer stretches of helical segments are observed.

e. Side-Chain Conformations. The conformational characteristics of the seven repeat unit aliphatic hydrocarbon side chain are analyzed in terms of its end-to-end distance. For that purpose, the distribution function of the end-to-end distance of each side chain in the 30 repeat unit PHD is analyzed for each MD simulation. The population shows a non-Gaussian behavior that is skewed toward longer chain lengths (data not shown). The skew is mainly due to the two double bonds that restrict rotations and bias extension. The optimum geometry of the dimer structure obtained by energy minimization, reported in the "analysis of the single chain" subsection, has a 7.6 Å end-to-end distance, which is an extended structure for the side chain. (The fully extended chain at its equilibrium bond lengths and angles would be ca. 7.7 Å.) Independent of temperature, environment, and the backbone conformation, we always observe extended side chains with end-to-end separation changing from 6.5 to 8.5 Å in all the MD simulations. However, unlike the findings from the molecular mechanics calculations of Marchessault et al.,[19] in the current MD simulations the bond between the extended side chain and the main chain does not have a preferred conformation that would lead to a herringbone conformation or a zigzag conformation of the polymer.

Conclusions

PHD is representative of a class of bacterial polyesters, PHAs, with desirable properties such as biodegradability, biocompatibility, and environmental compatibility. However, many of these polyesters are thermally unstable and display poor mechanical properties. It may be desirable to improve their bulk or surface properties by modifying their chemical structures, crosslinking, etc. Isotactic PHD is a good candidate for such treatment due to its long side chains that may be utilized for tuning the bulk or surface properties. Therefore, it is of utmost interest to understand the local structure of this system. In this study, the chain dimensions and conformational features of the PHD molecule are investigated using RIS calculations and MD simulations. The effects of the environment and temperature are examined in detail.

Experimental observations on PHB and our simulations of PHD exhibit similarities: (i) strong persistence for rodlike helices is observed in good solvent, and (ii) a sharp helix-to-coil transition is observed for both polymers in going from good to poor solvent conditions. Because of the presence of the large side chains, PHD shows Gaussian chain behavior with a nonzero mean end-to-end vector. In the vacuum environment, the chain dimensions are smaller than the unperturbed chain dimensions, whereas in chloroform they are larger. In fact, results from the vacuum simulations, RIS calculations, and chloroform simulations are representative of poor, Θ, and good solvent conditions, respectively, and they reflect the expected tendency of the characteristic ratio to increase as the solvent conditions are improved.

The populations of dihedral angles change as the temperature and/or environment change, except for those of the partially double bonded ester bond. In chloroform, chain conformations converge to the structure found from the optimization of PHD in a vacuum, which also corresponds to the lowest energy structure obtained in the RIS model.

The helix size and helix persistence in the simulations are related to the quality of the solvent. In poor solvents, PHD behaves like a random coil, while in good solvents a persistent rodlike shape is observed. However, because of the lack of hydrogen bonds and the small dipole moment of the ester compared to amino groups, the helix stability is expected to be lower than that of the proteins.[6] The side chains adopt a predominantly extended conformation irrespective of the environment and the backbone conformation. This feature makes PHD an excellent candidate for a bacterial polyester whose properties may be improved upon treatment.

References and Notes

(1) Cornibert, J.; Marchessault, R. H. *J. Mol. Biol.* **1972**, *71*, 735−756.
(2) Marchessault, R. H.; Yu, G.-e. In *Biopolymers*; Doi, Y., Steinbüchel, A., Eds.; Wiley: New York, 2002; Vol. 3b, pp 157−196.
(3) Avella, M.; Martuscelli, E.; Raimo, M. *J. Mater. Sci.* **2000**, 523−545.
(4) Pazur, R. J.; Raymond, S.; Hocking, P. J.; Marchessault, R. H. *Polymer* **1998**, *39*, 3065−3072.
(5) Brückner, A.; Meille, S.; Mallpezzi, L.; Cesaro, A.; Navarini, A.; Tombolini, R. *Macromolecules* **1988**, *21*, 967−972.
(6) Marchessault, R. H.; Okamura, K.; Su, C. J. *Macromolecules* **1970**, *3*, 735−740.
(7) Miyaki, Y.; Einaga, Y.; Hirosye, T.; Fujita *Macromolecules* **1977**, *10*, 1356−1364.
(8) Huglin, M. B.; Radwan, M. *Polymer* **1991**, *32*, 1293−1298.
(9) Beaucage, G.; Rane, S.; Sukumaran, S.; Satowski, M. M.; Schechtman, L. A.; Doi, Y. *Macromolecules* **1997**, *30*, 4158−4162.
(10) Sun, H. *J. Comput. Chem.* **1994**, *15*, 752−768.
(11) Sun, H. *Macromolecules* **1995**, *28*, 701−712.
(12) Flory, P. J. *Statistical Mechanics of Chain Molecules*; Wiley: New York, 1969.
(13) Andersen, H. C. *J. Chem. Phys.* **1980**, 2384−2393.
(14) Andersen, H. C. *J. Comput. Phys.* **1983**, 24−34.
(15) Allen, M. P.; Tildesley, D. J. *Computer Simulation of Liquids*; Oxford University Press: Oxford, 1987.
(16) Nosé, S. *Mol. Phys.* **1984**, *50*, 255−268.
(17) Flory, P. J. *Principles of Polymer Chemistry*; Cornell University Press: Ithaca, NY, 1953.
(18) Hedenqvist, M. S.; Bharadwaj, R.; Boyd, R. H. *Macromolecules* **1998**, *31*, 1556−1564.
(19) Marchessault, R. H.; Monasterios, C. J.; Morin, F. G.; Sundararajan, R. P. *Int. J. Biol. Macromol.* **1990**, *12*, 158−165.

MA021088Z